Polymer Bulletin 35, 457–464 (1995)

Polymer Bulletin

Atomic force microscopy of polyethylene and poly-(D-lactide) single crystals

K. Crämer[1], **A. Wawkuschewski**[1], **A. Domb**[2], **H.-J. Cantow**[1], **S. N. Magonov**[1]

[1] Freiburger Materialforschungszentrum und Institut für Makromolekulare Chemie, Universität Freiburg, Stefan-Meier-Strasse 21, D-79104 Freiburg, Germany
[2] Department of Pharmacy, The Hebrew University, Jerusalem, Israel

Received: 14 February 1995/Revised version: 13 April 1995/Accepted: 28 April 1995

Dedicated cordially to Prof. Dr. Joachim Klein to his 60th birthday

Summary

Single crystals of polyethylenes with different molecular weight and of poly(d-lactide) were examined with atomic force microscopy. Morphologies of single crystals and their aggregates formed by overlaying as well as multilayer crystals are shown. Elevated diagonals caused by sectorization were found on crystals of both polymers. The nanoscale images demonstrate a grain structure of the lamellar surfaces with lateral features in the 5-15 nm range and roughness of about 1 nm. Polyethylene and the polylactide crystals exhibit some additional directional surface structure. The results are discussed in terms of surface organization.

Introduction

Morphology and structure of polymer single crystals grown in dilute solutions are studied for a long time (1). The crystals appear as large lamellar platelets with lateral dimensions in the micron scale. A lamella is formed by multiple folding of polymer chains, with a thickness from 5 to 20 nm. Molecular folds are the structural elements of the lamellar surface. Though the main features of polymer crystals are known from optical and electron microscopy, the detailed structure of the lamellar surface is not wholly understood. Single crystals of linear and cyclic alkanes exhibit lamellar surface structures in agreement with their crystallographic data. This means a regular arrangement of methyl groups in the case of linear alkanes. In a cyclic alkane crystal, which can be considered as model for adjacent reentry in PE, the lamellar surface is formed by a lattice of molecular folds. These results were obtained by atomic force microscopy (AFM) of n-$C_{33}H_{68}$ and n-$C_{36}H_{74}$ as well as of $(CH_2)_{48}$ and $(CH_2)_{72}$ crystals (2). The lamellar surface of polymer crystals is expected to be more complex because polymer chains can form, besides adjacent reentry folds, switchboard-like connections of different length. Together with chain ends and - for multilayer crystals - tie molecules these elements form an amorphous phase.

Various experimental techniques were used to characterize the fold surface of polymer single crystals, among others density measurements, IR, NMR, SAXS, neutron scattering, and decoration techniques. The conclusions from different methods are not consistent concerning the portion of the different types of reentry. Recent model analyses indicate that, irrespective of crystallization conditions, the majority of chains of the fold surface is involved in tight folds (1). Nevertheless, the remaining varying sized loops take into account that according to density measurements - especially by SAXS (3) - the fold layer appears as an amorphous component, on an overall scale. On the base of calorimetric and of NMR measurements a third constrained or "rigid amorphous" phase was distinguished, that led to a three-phase model (4).

PE crystals grow as hollow pyramids in solution. They accomodate flat geometry, i. e. lozenge-shaped platelets, being deposited on the substrate. Bright and dark field electron microscopy revealed distinct sectors defined by the lozenge diagonals. The molecular orientations within neighboring sectors are inclined to each other. The sectors are related to the different pyramid faces (5). Progress in the characterization of the fold surface was achieved by decoration techniques (1). An epitaxial layer formed by deposited vapor of polymer fragments exhibits different orientation in different sectors. A more direct approach providing local information of the fold surface can be expected by the scanning probe techniques.

During the last years scanning tunneling microscopy, STM, and AFM were established as powerful surface methods with expanding applications to polymers . First AFM studies on single crystals of PE and of polyethyleneoxide were limited, however, to observations of their basic morphology (6). In a STM study of metal-coated PE crystals fine structural details were found with some limitations related to the decoration (7). Recently a molecular-scale image of the lamellar PE surface that resembles adjacent reentry fold order was reported (8).

An AFM study of single crystals of different molecular weight PE and of poly(d-lactide) - PDLA - is presented below. Crystal imaging was conducted in different modes in air and under water in order to obtain reliable images revealing surface features in the 1 - 100 nm range (9).

Experimental

Single crystals of PE with $M_w = 4,5 \cdot 10^3$ ($M_w/M_n=4.1$, Vestowax A409, Hüls AG) and with $M_w = 6.7 \cdot 10^4$ $gmol^{-1}$ ($M_w/M_n=7.5$, Hoechst AG) were grown in .01 % xylene solutions at 85° C for several days. One drop of solution was deposited on a mica substrate and dried.

The poly(D-lactide) was grown from a acetonitril solution by cooling down from 80° C to room temperature within several hours. The monomer - DLA - has been synthesized, and the polyreaction has been performed to $M_w = 1.28 \cdot 10^5$ gmol^{-1}(M_w/M_n=1.86).

A scanning probe microscope Nanoscope III (Digital Instruments Inc.) was used in this study. Rectangular Si cantilevers (Nanoprobes) were applied for the contact and tapping mode experiments. Simultaneous registration was performed - in the contact mode (CM) for the heigth (HT) and the normal deflection (DF) images, or for the HT and the lateral force (LF) images - and in the tapping mode (TM) for the HT and the amplitude (AM) images. AM represents mainly the height derivative values.

The lamellar surfaces were stable enough for imaging in air and water at moderate forces. Even in the best resolved images obtained in sub-water measurements (9) convolution of the probe apex shape with surface features occurs. Though we chose the most characteristic images from experiments with different probes, lateral feature dimensions can be overestimated, especially in ambient condition studies. This effect should be considered particularly for imaging of single lying objects with nanoscale dimensions (10). However, the size of those elements within compact layers can be detected more precisely (9).

Results

After depositing polymer solution on mica and drying, the sample was examined with an optical microscope. AFM measurements were conducted close to surface regions where large crystals and their aggregates were found. Single crystals of low molecular weight PE are shown in Fig. 1a. The crystals exhibit lozenge shape with an acute angle of about the ideal value of 67.5°. The topographical profile along the cross-section line A-A (upper part of Fig. 1a) indicates an uniform thickness of ca. 10 nm within the central part of the lamella. A frame-type thicker region of ca. 0.5 µm in width is seen at the crystal borders outmost surrounded by an unstructured thinner layer. Because the crystallization of polymer lamellae proceeds laterally, the border regions can be assigned to the crystallization front. The outmost thin layer is related probably to less-crystalline material that is expelled from bulk during crystallization. This is plausible by the fact that this layer exhibits inferior mechanical stability in the AFM experiment compared with the single crystal. The nature of the thicker border regions, which were not found on all crystals, is not clear.

The surface plot (Fig. 1c) of overlapping crystals, Fig. 1b, exhibits sharp steps. This can be explained as shearing of the top platelet (2, resp. 3, see Fig. 1b,c) into two parts by slipping along the vertical c-axis at the edge of the underlying crystal (1, resp. 2). Slippage of PE chains along the c-axis is plausible energetically (11). The pyramid-lozenge flattening process of PE crystals, and the formation of spiral multilayer crystals by screw dislocation mechanisms (12) are related to similar elementary processes. Two spirals with terraces separated

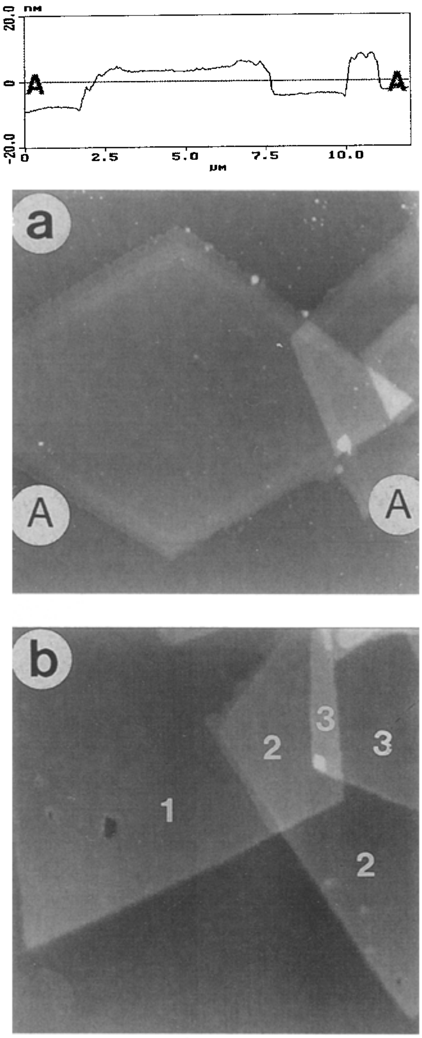

by vertical 10 nm steps are shown in Fig. 2. They grow by a simple (Fig. 2a) or double screw dislocation mechanism (Figs. 2b, c). The lamellar surface of the first terrace in Fig. 2a exhibits oriented features of about 60 nm width (indicated by an arrow).

Our study shows that with AFM one can directly distinguish surface features related to the sectorization of the PE crystal. Though the lamellar surface looks smooth except the border regions, in some crystals we found 15-20 nm wide elevated striations lying along the lozenge diagonals, Figs. 3a-b. They divide the PE crystal in four sectors reflecting the misfit planes between these sectors with different molecular orientation. Relaxation during pyramid collapse is probably more hindered with an increase of molecular weight. This explains the fact that we observed sectorization borders only in the crystals of higher molecular weight. In another crystal shown in Fig. 3c we found several striations spreading from the centre of the platelet, as indicated by arrows in the zoomed image, Fig. 3d. These misfit borders indicate

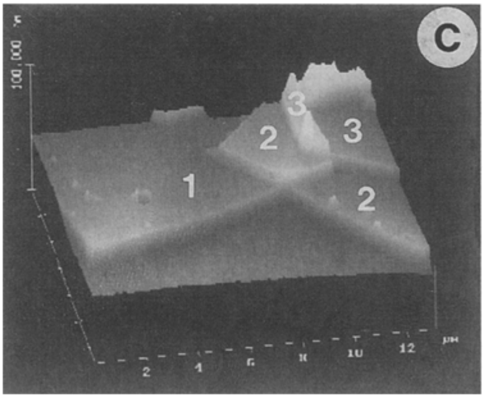

Figure 1: (a) AFM TM-HT image in air of single PE crystals ($M_w = 4.5 \cdot 10^3$). Cross-section A-A profile is indicated in the upper part of the picture, area 12.0 x 12.0 µm. The image contrast indicates height variations in the 0-40 nm range • (b) AFM CM-HT image in air of overlaying PE crystals ($M_w = 4.5 \cdot 10^3$), area 13.0 x13.0 µm
• (c) Surface plot of Fig. 1b

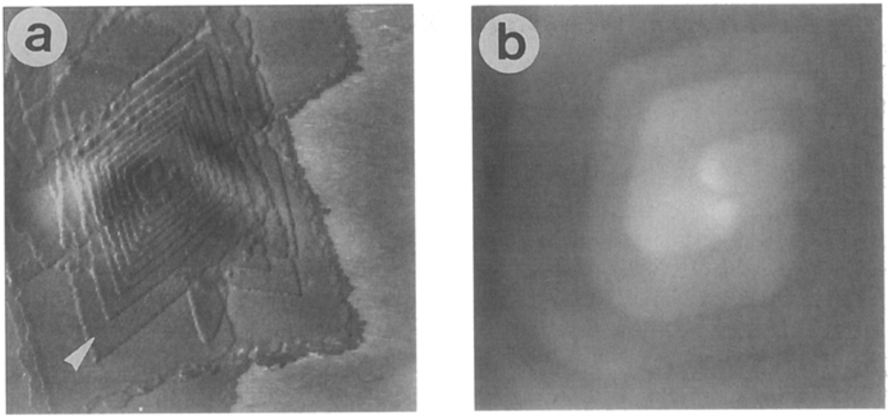

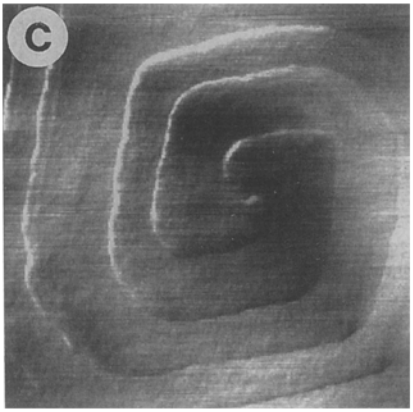

Figures 2: (a) AFM CM-DF image in air of a PE spiral with single screw dislocation ($M_w = 4.5 \cdot 10^3$), area 6.0 x 6.0 µm^2
• (b)-(c) AFM CM-HT and CM-DF images under water of PE spirals with double screw dislocation ($M_w = 6.7 \cdot 10^4$), area 1.0 x 1.0 µm^2
Contrast in the height image (b) indicates variations 0-70 nm

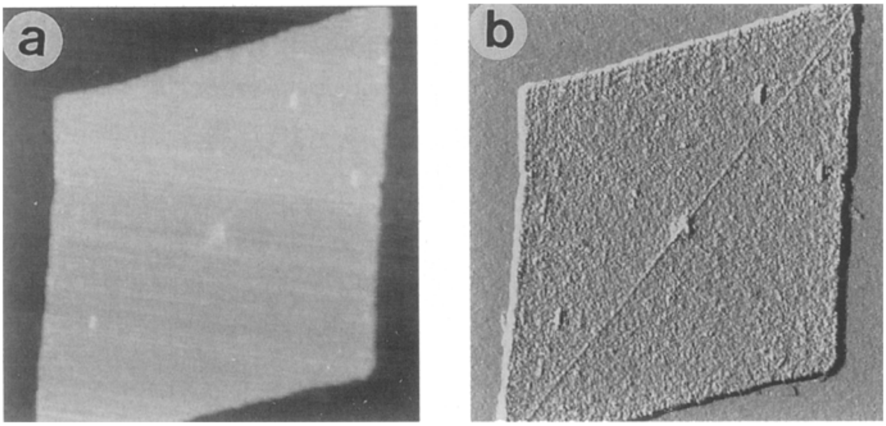

Figures 3: (a, b) AFM TM-HT and TM-AM images in air of a PE single crystal ($M_w = 6.7 \cdot 10^4$), area 2.5 x 2.5 µm^2

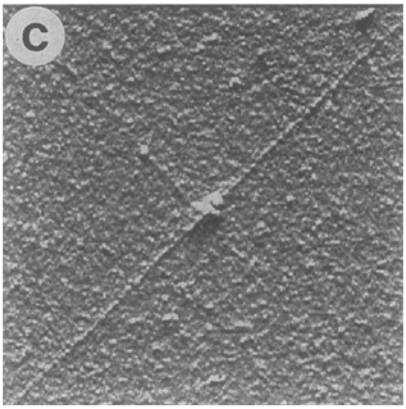

Figures 3: (c) A zoomed 1.5 x 1.5 μm^2 part of the TM-AM image (b). The image contrast indicates height variations 0-20 nm

- (d) TM-AM image of PE crystals in air ($M_w = 6.7 \cdot 10^4$), area 5.0 x 5.0 μm^2
- (e) A zoomed 1.0 x 1.0 μm^2 part of the image in (d).

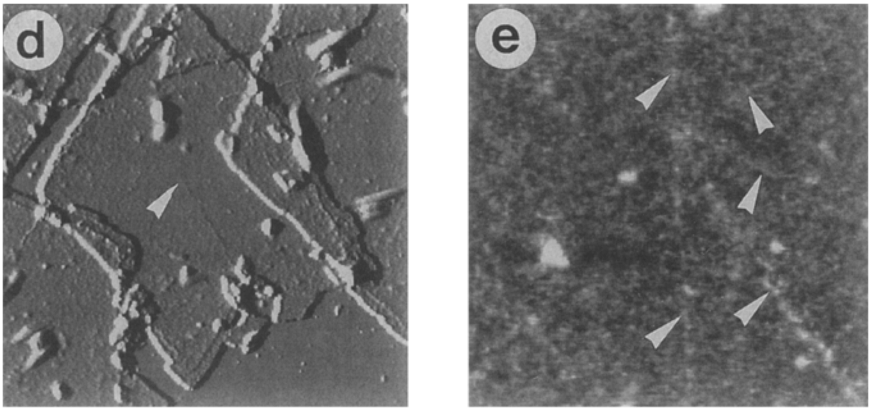

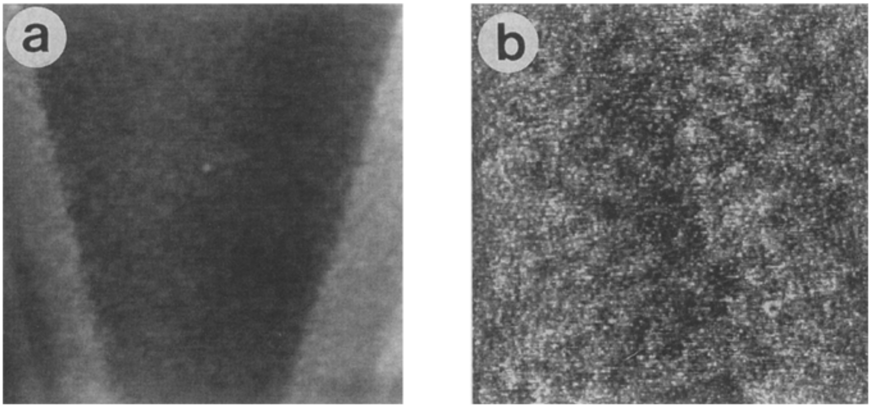

Figures 4: (a) AFM TM-HT image in air of the edge of a PE crystal ($M_w = 4.5 \cdot 10^3$), area 1.25 x 1.25 μm^2 - (b) TM-HT image in air of the central part of the PE crystal in Fig. 1a, area 1.0 x 1.0 μm

on a complex crystal structure that might consist of several microsectors (13) with different molecular order.

To describe the nanostructure of the lamellar surface we consider the high magnification AFM images. Fig. 4a shows a surface region at the crystal corner that reveals a similar grain-like structure of the central part and of the thicker borders. This structure is common to the PE crystals of both molecular weights. Figure 4b demonstrates a central part of the surface of a low molecular weight PE crystal in Fig. 1a. It shows ordering of small grains of 10-15 nm in diameter into large assemblies of 70-80 nm. The small grains were found in all samples. The large patterns, however, were seen only in some crystals. The related surface roughness is ca. 1 nm. In some cases a fine substructure with features in the 5-7 nm range was found. Grain structure and sector borders remain essentially unchanged in measurements with different forces. Hence, the observed features cannot be assigned to locally different surface hardness, but to topography. They are not related to physisorbed or to weakly bound material, because they were not removed in high-force experiments.

The AFM results indicate that the lamellar surface of PE crystals contains "rigid amorphous" material (4c). This agrees with results of density measurements on PE crystals (1). The surface grain structure can be explained by locally variant protrusions of chain stems in the adjacent reentry model and by presence of loose chain ends and loops, i. e. local switch-board character.

The main features of PE single crystals were also found in the images of the PDLA crystals. Here also lozenge shape crystals have been found, Fig. 5. Sector borders have been observed, however, along the long diagonal only. In the sectors one can see directional patterns of about 20-30 nm in size. Ordered features of similar scale

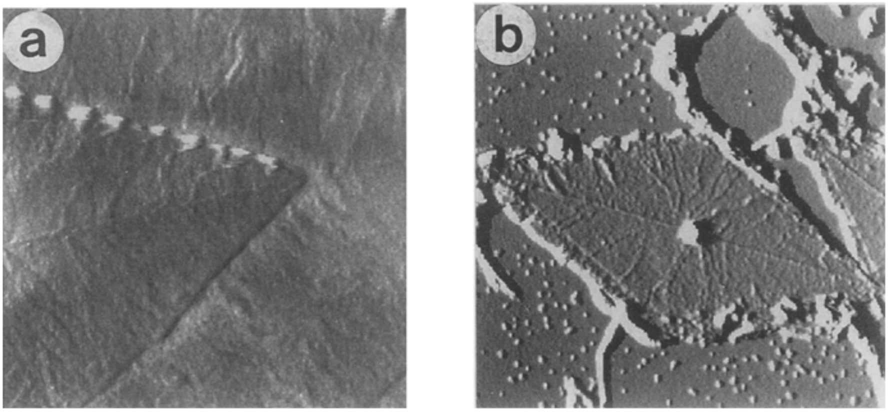

Figures 5: (a) AFM TM-AM image in air of a PDLA crystal aggregate, area 1.2 x 1.2 μm^2 • (b) TM-AM image in air of a PDLA single crystal, area 5.0 x 5.0 μm^2

were found on the PE crystal in Fig. 2a. They may be related to peculiarities of pyramid flattening. But, the existence of pyramids is not proved for the polylactide crystals up to now. Grains of 10-15 nm in diameter are the smallest elements distinguished on the lamellar surface of the PDLA. Measurements at higher force indicated that the crystals exhibit high rigidity, comparable with that of PE crystals.

To summarize, by examining the PE and PDLA crystals with AFM we detected surface features related to crystal sectorization and a grainy and rigid amorphous nanostructure of the lamellar surfaces. These results differ from the recent observation of molecular-scale ordered AFM images on the lamellar PE surface (8). These images were presented as evidence of adjacent reentry of fold surface organization. On the amorphous a-b-surface of PE and polylactide crystals molecular-scale order was not detected. The striation pattern on the PDLA crystal, however, may give some indication on the average loop orientation. The answer, whether there is a common type of surface order in semicrystalline polymers, will be given by systematic studies of lamellar surfaces with AFM as the suitable method for this purpose.

Acknowledgments • We acknowledge Prof. Dr. J. Petermann of the Universität Dortmund and D. Brizzolara from the Institut für Makromolekulare Chemie Freiburg for the discussion of AFM results.

References

1. Recent review: Lotz B, Wittmann JC (1993) in "Structure and Properties of Polymers" Thomas E (ed.) p. 79, VCH Weinheim
2. Stocker W, Bar G, Kunz M, Möller M, Magonov SN, Cantow H.-J. (1991) Polym Bull *26*:215
3. Fischer EW, Kloos F (1970) J Polym Sci B8:865
4. (a) McBrierty VJ (1979) Disc Faraday Soc 68:310
   (b) Mandelkern L (1979) Disc Faraday Soc 68:310
   (c) Grebowicz J, Varma-Nair M, Wunderlich B (1992) Polym Adv Tech 3:51
5. (a) Patil R, Kim S-J, Smith E, Reneker DH, Weisenhorn AL (1991) Polym Comm 31:455
   (b) Snetivy D, Vansco GJ (1992) Polymer 33:432
6. Niegisch R, Swan PR (1960) J Appl Phys 31:1906
7. Piner R, Reifenberger R, Martin DC, Thomas EL, Apkarian RP (1990) J Polym Sci Polym Lett 28:399
8. Patil R, Reneker DH (1994) Polymer 35:1909.
9. Wawkuschewski A, Crämer K, Cantow H-J, Magonov SN (1994) Ultramicroscopy submitted
10. Radmacher M, Fritz M, Hansma HG, Hansma PK (1994) Science 265:1577
11. Shadrake LG, Guiu F (1979) Phil Mag 39A:785
12. Frank FC, Keller A, O'Connor A (1959) Phil Mag 4:200
13. Bassett DC (1981) in "Principles of Polymer Morphology" Cambridge Univ Press 72-60